IN-57
31642
38 P

NASA Technical Memorandum 109152
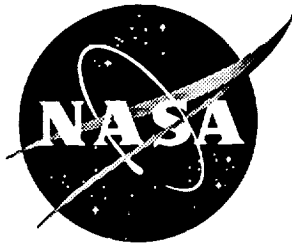
Wind-Tunnel Blockage and Actuation Systems Test of a Two-Dimensional Scramjet Inlet Unstart Model at Mach 6

Scott D. Holland
Langley Research Center, Hampton, Virginia

November 1994

Summary

The present study examines the wind-tunnel blockage and actuation systems effectiveness in starting and forcibly unstarting a two-dimensional scramjet inlet in the NASA Langley 20-Inch Mach 6 Tunnel. The intent of the overall test program is to study (both experimentally and computationally) the dynamics of the inlet unstart; however, prior to the design and fabrication of an expensive, instrumented wind-tunnel model, it was deemed necessary first to examine potential wind-tunnel blockage issues related to model sizing and to examine the adequacy of the actuation systems in accomplishing the start and unstart. The model is equipped with both a moveable cowl and aft plug. Following the injection of the model into the freestream, the cowl is raised and lowered to allow the inlet to start. The plug located in the exit plane is then rapidly driven forward to decrease the exit area and force the inlet to unstart. Schlieren windows in the inlet sidewalls allow limited optical access to the internal shock structure and permit the identification of model start and unstart. For this blockage test, a video camera was incorporated into the schlieren system to record the schlieren of the entire start/unstart sequence on VHS video tape. The framing rate and shutter speed of the camera were too slow to fully capture the dynamics of the unstart but did prove sufficient to identify start/unstart. A chronology of each actuation sequence is provided in tabular form along with still frames from the schlieren video. A pitot probe monitored the freestream conditions throughout the start/unstart process to determine if there was a blockage effect due to the model start or unstart. Because the purpose of this report is to make the phase I (blockage and actuation systems) data rapidly available to the community, the data is presented largely without analysis of the internal shock interactions or the unstart process. This series of tests indicated that the model was appropriately sized for this facility and identified operability limits required first to allow the inlet to start and second to force the unstart.

Symbols

a_e inlet exit area, sq. in.
a_t throat area, 5.16 sq.in.
M_∞ freestream Mach number
p_∞ freestream static pressure, psia
$p_{t,1}$ tunnel stagnation pressure, psia
$p_{t,2}$ freestream pitot pressure, psia
Re_∞ unit freestream Reynolds number, ft^{-1}
T_∞ freestream static temperature, °R
$T_{t,1}$ tunnel stagnation temperature, °R
x,y,z axial, lateral, and vertical Cartesian coordinates (respectively) , inch

Conventions

The model is injected into the tunnel oriented inverted with respect to flight, i.e. the cowl is shown in the top of the images. *Up* and *down* shall be defined with respect to the model such that cowl up indicates the configuration with maximum throat area, and cowl down indicated the configuration with minimum throat area. Therefore, the cowl is moved *upward* to aid in inlet starting.

Introduction

The present work examines the wind-tunnel blockage and actuation systems effectiveness in starting and forcibly unstarting a two-dimensional scramjet inlet in the NASA Langley 20-Inch Mach 6 Tunnel. The intent of the overall test program is to study the dynamics of the inlet unstart via both computational and experimental techniques. This work was initiated in conjunction with a CFD effort at North Carolina State University, wherein time-accurate calculations of a back-pressure induced inlet unstart were made. CFD was used in the preliminary design of the 2-D scramjet inlet configuration. Because of the complexity and high speed with which the unstart takes place (on the order of 15ms, based on preliminary CFD results), a blockage model has been designed and fabricated (prior to the design of an expensive instrumented wind-tunnel model) first to address wind-tunnel blockage issues related to model size/interference and second to examine the adequacy of the actuation systems in accomplishing the start and unstart. A follow-on phase is planned (funding permitting), in which the dynamics of the unstart will be investigated; this second phase will make use of high-speed schlieren movie cameras and high-frequency instrumentation.

The model is equipped with both a moveable cowl and aft plug. Following the injection of the model into the freestream, the cowl is raised and lowered to allow the inlet to start. The plug (located in the exit plane) is then rapidly driven forward to decrease the exit area and force the inlet to unstart. Schlieren windows in the inlet sidewalls allow limited optical access to the internal shock structure and permit the identification of model start and unstart. For this blockage test, a video camera was incorporated into the schlieren system to record the schlieren of the entire start/unstart sequence on VHS video tape. (Copies of the video may be obtained separately as Video Supplement L-0194-41 to NASA TM 109152.) The framing rate and shutter speed of the camera were too slow to fully capture the dynamics of the unstart but did prove sufficient to identify start/unstart. Frames from the video tape are included in this report as still images along with tables which provide the actuation sequence for each run. A pitot probe monitored the freestream conditions throughout the start/unstart process to determine if there was a blockage effect due to the model start or unstart.

Because this report documents the first phase of the overall test program (namely, blockage and actuation systems tests), the discussion is limited to these topics; hence, no analysis is presented with respect to the origin or nature of the unstart phenomena in this report. In particular, the following questions related to the wind-tunnel blockage and actuation systems are addressed as the primary focus.

1. For a given freestream Reynolds number and plug configuration, will the inlet start through any combination of surface movement?

2. If the inlet can be started, is the throw on the aft plug sufficient to force the unstart?

3. If the inlet can be started and unstarted, will the inlet restart by simply retracting the plug (i.e., is the inlet self-starting)?

4. If the inlet can be started and unstarted, will the inlet restart by cycling the cowl after the plug is moved aft?

5. Will the inlet (configured with the plug aft and the cowl down) start solely due to model injection (i.e., will the model pulse start)?

6. Does the tunnel unstart or exhibit partial blockage effects (change in freestream conditions) as a result of model injection, model start, or model unstart?

Experimental Techniques

Model Description

A dimensioned sketch of the inlet model is shown in Figure 1. The geometry consists of a 15° ramp (8.85 inches long by 7.00 inches wide), a circular arc sector (4.623 inch radius), a 10° expansion (2.15 inches long), a constant area section (1.5 inches long), and a 20° expansion (0.687 inch long). The cowl leading edge is located 7.511 inches aft of the ramp leading edge. The minimum throat height is 0.7373 inch, yielding a minimum throat area (a_t) of 5.16 sq.in. Both the cowl and the aft plug are actuated during the run using air cylinders supplied by 150 psi supply air lines. Following model injection into the freestream, the cowl is cycled to allow the inlet to start. At its maximum travel, the cowl rotates upward by almost 6° to increase the minimum throat height to 1.442 inches. After the cowl has been returned to its initial position and the inlet has started, the aft plug is driven forward to force the inlet to unstart.

The wedge-shaped plug has a 20° half-angle, a maximum thickness of 1.182 inches, and spans the entire 7.0 inch exit width. The plug is equipped with a removable shim (0.5 inch thick), which permits initial plug leading-edge positions 14.5 in and 15.0 in downstream of the ramp leading edge; the forward throw of the plug is one inch. Without the shim, the ratio of exit to throat area a_e/a_t is 1.33 and 0.86 for the plug aft and forward, respectively; with the shim, 1.10 and 0.63, respectively.

The model is fabricated of 15-5PH, H1025 stainless steel. Two sets of schlieren-quality BK-7 glass installed in the inlet sidewalls provide optical access to the throat and plug regions.

Description of Wind Tunnel Facility

The facility used for the present study was the 20-Inch Mach 6 Tunnel, located at the NASA Langley Research Center. A description of the tunnel and tunnel performance characteristics can be found in Ref. 1, of which the following is a summary. Figure 2 presents a schematic of the facility. Dry air is supplied from a 600 psia, 42000 ft^3 reservoir and heated to a maximum of approximately 1000°R. The air passes through a dryer and 5 micron filter before entering the settling chamber, which contains a perforated conical baffle and internal screens. The flow is expanded through a fixed-geometry, two-dimensional contoured nozzle (0.399 in x 20 in throat) into a 20.5 in x 20 in test section. The nozzle length from the center of the test section window to the throat is 7.45 ft. The model is supported on an injection system which inserts the model into the flow from below. Due to the run time of this facility (up to 15 minutes for certain conditions), it is possible to have multiple model injections per run, either at the same run conditions (for repeatability) or at different run conditions.

Test Conditions and Test Matrix

Nominal test conditions for the present test were chosen to provide as large a range of Reynolds numbers as possible and to coincide with conditions for which previous facility calibrations had been performed. Tests were performed at Mach 6 for nominal reservoir pressures of 30, 125, 250, and 475 psia at a nominal reservoir temperature of 910°R, corresponding to nominal freestream unit Reynolds numbers of 0.5, 2.1, 3.9, and 7.1 million/ft, respectively. Pitot pressure at the test section was measured for each run to serve as an indicator of tunnel blockage. Representative flow conditions (see Ref. 2) are presented in Table 1.

Table 1: Flow Conditions

$P_{t,1}$ (psia)	$T_{t,1}$ (°R)	p_∞ (psia)	T_∞ (°R)	q_∞ (psia)	M_∞	Re_∞ million/ft	Test Core (in)
31	866	0.0249	113.1	0.580	5.77	0.638	13x12
122	911	0.0830	113.5	2.041	5.93	2.175	13x13
241	933	0.1544	114.4	3.874	5.99	4.045	14x14
485	932	0.2895	111.7	7.437	6.06	7.959	14x16

The test matrix was constructed to test at each chosen flow condition both with and without the plug shim and to allow for repeat runs. Table 2 presents the test matrix. (Note again that due to the long run times of the facility, multiple injections are possible within one run, hence the need for both run and injection number in the table.) Because the facility shares vacuum spheres and air supply with other facilities, often the order in which the runs are made is determined by a combination of factors (including the desired test condition and vacuum sphere availability and pressure) in order to enhance facility productivity.

Table 2: Test Matrix/Run Log

Run Number	Injection Number	$p_{t,1}$ (psia)	Re_∞ (million/ft)	Plug Configuration
1	1	30	0.5	with shim
	2	100	1.8	with shim
	3	100	1.8	with shim
2	1	100	1.8	without shim
	2	100	1.8	without shim
	3	250	3.6	without shim
	4	250	3.6	without shim
3	1	30	0.5	without shim
	2	30	0.5	without shim
	3	30	0.5	without shim
	4	125	2.1	without shim
	5	125	2.1	without shim
	6	250	3.9	without shim
	7	250	3.9	without shim
	8	475	7.1	without shim
	9	475	7.1	without shim
4	1	30	0.5	with shim
	2	30	0.5	with shim
	3	125	2.2	with shim
	4	125	2.2	with shim
	5	250	3.9	with shim
5	1	475	7.1	with shim

Results

A chronology of each model injection sequence is presented in tabular format in the appendix. Because of the degradation in quality during the frame-grabbing process, the still images taken from the video did not reproduce well. Thus only a selected sampling of these still frames is presented, and the reader is referred to the video supplement. (Flow is from right to left, and the inlet is oriented with the cowl on top.) The video possesses higher quality images which provide a better view of the shock structure for started and unstarted configurations along with at least a sense of the flow dynamics, of which only brief notations are made in the tables. In the video, the plug motion is obvious because the plug is visible in the aft window. The cowl motion, however, is not as obvious because the cowl is hidden by the inlet sidewall. The end of the cowl actuator arm, however, becomes visible above the top of the inlet sidewalls between the windows when the cowl is up. (See Figure 1b.)

Table 3 presents a summary of the inlet starting behavior for each Reynolds number and plug configuration. Terms used in the table are defined as follows. *Starting* was identified as the establishment of an oblique shock structure inside the inlet, as observed in the video. Also, when the inlet started, the shock on the outboard side of the cowl (visible above the inlet) was attached and steady. The internal flow field additionally appeared steady. *Self-starting* indicates that the inlet will start without a change in throat area. This is determined by unstarting the inlet by the forward plug motion and observing whether the inlet restarts when the plug is returned to its aft position. Self-starting is a significant feature in an inlet design because it indicates that variable geometry is not necessary to restart the inlet. *Pulse-starting* indicates that the inlet would start when injected (with the cowl down) into the tunnel without actuation of any surface, i.e., the inlet starts due to the ram effect of the freestream as the model is thrust into the flow. Pulse-starting may be significant in situations where the inlet is shrouded for a portion of the flight trajectory, because shroud separation may effectively pulse-start an inlet in flight. Pulse-starting is also significant for these tests because it determines whether the added expense of a cowl actuation system is required for the Phase II of this study (the instrumented model to be designed pending the results of this blockage and actuation systems test).

Table 3: Summary of Inlet Starting Behavior

Reynolds Number	Plug Configuration	Starts	Self-starts	Pulse-starts
0.5 million/ft	without shim	no	no	yes
	with shim	no	no	--
2 million/ft	without shim	yes	no	no
	with shim	no	no	no
3.9 million/ft	without shim	yes	no	no
	with shim	yes	yes	--
7.1 million/ft	without shim	yes	yes	yes
	with shim	no*	--	no

* Only one run was obtained at this condition, and due to plug actuation problems, this result is in question, i.e., the failure of the model to start is believed to be due to a malfunction of the plug actuation system.

The ability of the inlet to start at Mach 6 in any configuration appears to be significantly Reynolds number dependent. At Re=0.5 million/ft, the inlet would not start for any configuration during any sequence of plug/cowl actuation, save one pulse-start when injected with the cowl down. (This pulse start could not be subsequently repeated, and the cause is unclear.)

At Re≈2 million/ft, the inlet starting behavior is dependent upon plug configuration. Despite the fact that for the plug in the aft position, the ratio of exit to throat area remained greater than unity with the shim (a_e/a_t=1.10), the inlet would not start, whereas for the plug configured without the shim (a_e/a_t=1.33), the inlet would start. For this configuration, the inlet would start only by cycling the cowl up and then down, and then once unstarted by the plug, the inlet would not restart (self-start) when the plug was retracted.

At Re=3.4 million/ft, inlet starting was no longer governed by the plug configuration and the inlet would start when the cowl was cycled up and then down. The inlet would not pulse-start, yet for one injection (Run 4, Injection 5 --- Table A.21), the inlet would repeatably restart (self-start) when the plug was retracted. Oddly, this occurred for the plug configured with the shim and not for the plug configured without the shim. This is a nonintuitive result; unfortunately, as a blockage model, the model was not instrumented, and no data on, for example, wall surface temperature or back pressure was available for a conjecture to be put forth as to the cause.

At Re=7.1 million/ft, the inlet reliably started and restarted (self-started) for plug forward and aft movement, respectively, for the plug configured without the shim. The inlet also pulse-started at this Reynolds number. Sample frames from started and unstarted inlet configurations are presented in Figures 3 and 4, respectively, for Re=7.1 million/ft with the plug configured without the shim. Despite the poor reproducibility of the image, the difference between start and unstart is clear. In addition to the lack of a clearly-defined oblique shock structure inside the unstarted inlet of Figure 4, the external influence of the unstart is significant (due primarily to spillage around the cowl). The large external influence, however, was not large enough to unstart the tunnel or partially block the facility, as inferred from a pitot probe located below the inlet which monitored freestream conditions. Figure 5 shows (on a relatively fine scale) the measured pitot pressure throughout Run 3/Injection 8 (Re=7.1 million/ft), overlaid with the actuation signals to indicate the position of the plug and cowl. Figures 6-9 show similar results for each of the other Reynolds numbers at which the model was tested, including configurations with and without the plug shim. The plots illustrate that the inlet start and unstart process did not induce partial blockage effects on the facility (as inferred from pitot measurements), and hence that the model was appropriately sized for the facility.

Although the primary purpose of this phase of the study is satisfied by the determination of the absence of blockage effects, some comments regarding the flow field structure are appropriate. Frame by frame advancement of the video illustrates that when the inlet is not started, the flow field is fully three-dimensional and unsteady. The multiple curved shock images external to the cowl suggest a rippled shock with intermittent spillage across the span of the inlet. When the inlet starts, the flow field appears to become nominally two-dimensional, with crisp, singular images of the steady attached oblique shocks, both internal and external to the inlet.

Preliminary computational work (performed by Rusty Benson at NCSU in May 1993) suggests that the mechanism for the unstart is a separation which moves forward of the throat. Similar Mach 3 results have been presented in Ref. 3 for a back-pressure induced unstart. (See, for example, Figure 5.28 of Ref. 3.) Figure 10 is a still frame from the schlieren video

at unstart. Results from the previously noted computational work indicate that the shock interacting with the cowl shock in the forward window may emanate from a separation on the forebody plane upstream of the throat. If the unstart is indeed separation driven, then increased Reynolds number appears to minimize the size and extent of the separation, which may allow the inlet to restart when the plug is returned to its aft position.

Concluding Remarks

The present work examined the wind-tunnel blockage and actuation systems effectiveness in a generic two-dimensional scramjet inlet as a first phase in a test program designed to study the dynamics of inlet unstart. An inexpensive, uninstrumented wind-tunnel model was tested in the NASA Langley 20-Inch Mach 6 Tunnel to examine the wind-tunnel blockage issues related to model sizing and to examine the adequacy of the actuation systems in accomplishing the start and unstart. The model was equipped with both a moveable cowl and aft plug. Following model injection, the cowl was raised and lowered to allow the inlet to start. The plug (located in the exit plane) was then rapidly driven forward to decrease the exit area and force the inlet to unstart. Schlieren windows in the inlet sidewalls allowed limited optical access to the internal shock structure and permitted identification of model start and unstart. For this blockage test, a video camera was incorporated into the schlieren system to record the schlieren of the entire start/unstart sequence on VHS video tape (available separately as Video Supplement L-0194-41 to NASA TM 109152). The framing rate and shutter speed of the camera were too slow to fully capture the dynamics of the unstart but did prove sufficient to identify start/unstart. A pitot probe was placed beneath the inlet to

identify any influence of the start/unstart process on the local freestream conditions.

The conclusions from this study may be summarized as follows.

1. The ability of the inlet to start at Mach 6 appears to be significantly Reynolds number dependent. At Re=0.5 million/ft, the inlet would not start for either the plug configured with or without the shim; however, inlet starting steadily improved with increasing Reynolds number.

2. The one inch throw of the aft plug (which reduced the ratio of exit to throat area from 1.33 to 0.86 for the plug configured without the shim and from 1.10 to 0.63 for the plug configured with the shim) was sufficient to force the inlet to unstart.

3. Self-starting was observed only at the highest Reynolds numbers. Preliminary computational findings suggest that the mechanism for the unstart is a separation which moves forward of the throat. If the unstart is indeed separation driven, then increased Reynolds number appears to minimize the size and extent of the separation, which may allow the inlet to restart when the plug is returned to its aft position.

4. For configurations which were not self-starting, cycling the cowl up and down after the plug is moved aft was generally sufficient to restart the inlet, i.e. no additional mechanism such as bleed was necessary to restart the inlet.

5. Pulse-starting (the ability of the inlet to start due to model injection without variable geometry on the cowl) was observed for only two configurations; thus, the cowl actuation system remains a requirement for future testing.

6. The tunnel remained started during each sequence of model injection, model

start, and model unstart and, based on measured freestream pitot pressures, exhibited no partial blockage effects (change in freestream conditions) as a result of the sequences.

In summary, this series of tests indicated that the model was appropriately sized for this facility and identified operability limits required first to allow the inlet to start and second to force the unstart.

NASA Langley Research Center
Hampton, VA 23681-0001
August 29, 1994

References

1. Miller, C. G., III: Langley Hypersonic Aerodynamic/Aerothermodynamic Testing Capabilities - Present and Future. AIAA 16th Aerodynamic Ground Testing Conference, June 18-20, 1990, Seattle, WA, AIAA-90-1376.
2. Miller, C. G. and Smith, F. M.: Langley Hypersonic Facilities Complex - Description and Application. AIAA 14th Aerodynamic Testing Conference, March 5-7, 1986, West Palm Beach, FL, AIAA-86-0741-CP.
3. Benson, Rusty A.: Development of a Time-Accurate Algorithm Coupled with a Dynamic Solution-Adaptive Grid Algorithm with Applications to Generic Inlet/Diffuser Configurations. Ph.D. Dissertation, North Carolina State University, 1994.
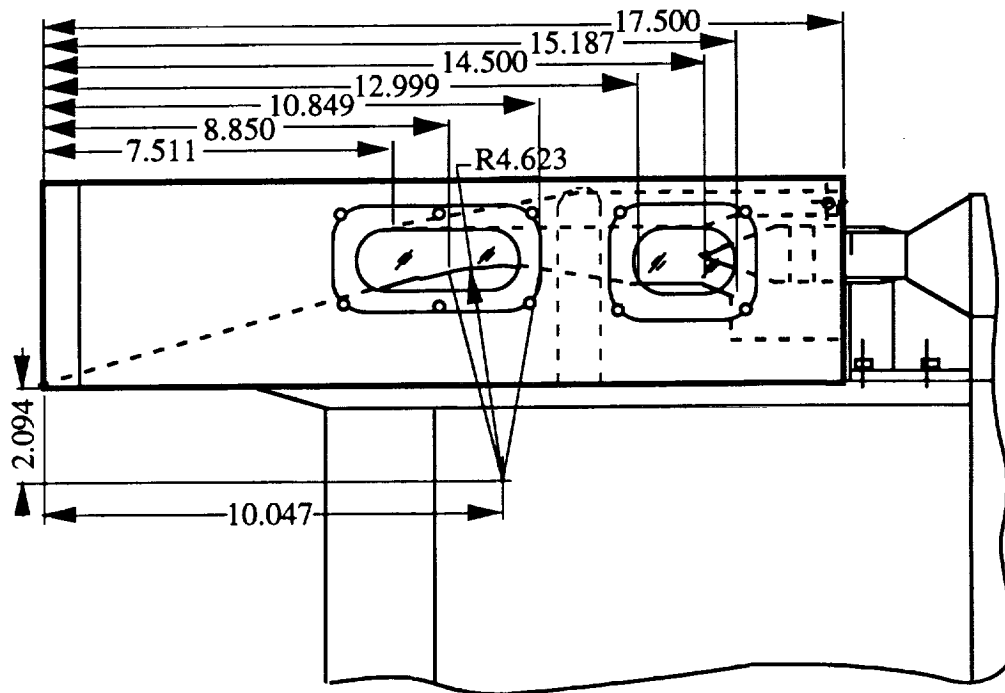
(a) Dimensioned Sketch (All dimensions in inches)
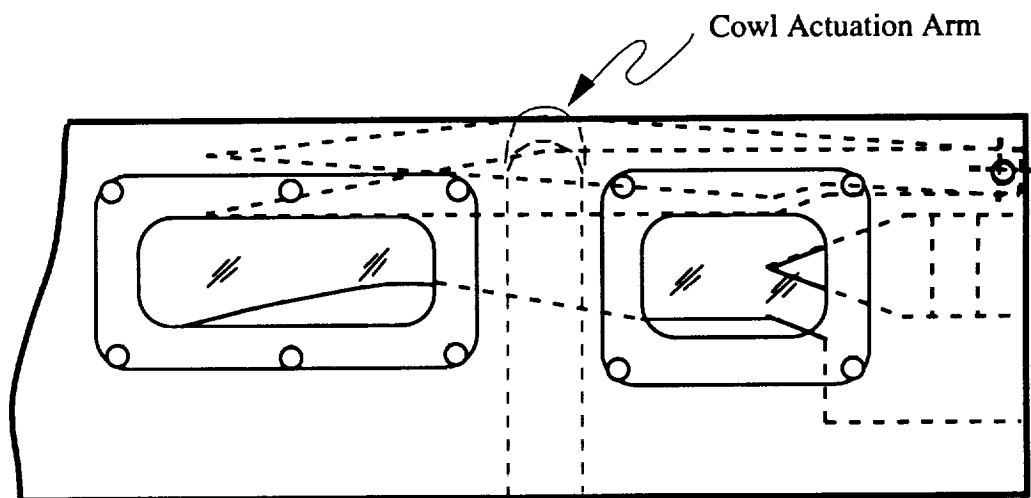
Cowl Actuation Arm

(b) Sketch of Cowl Actuation Arm With Cowl Raised and Lowered
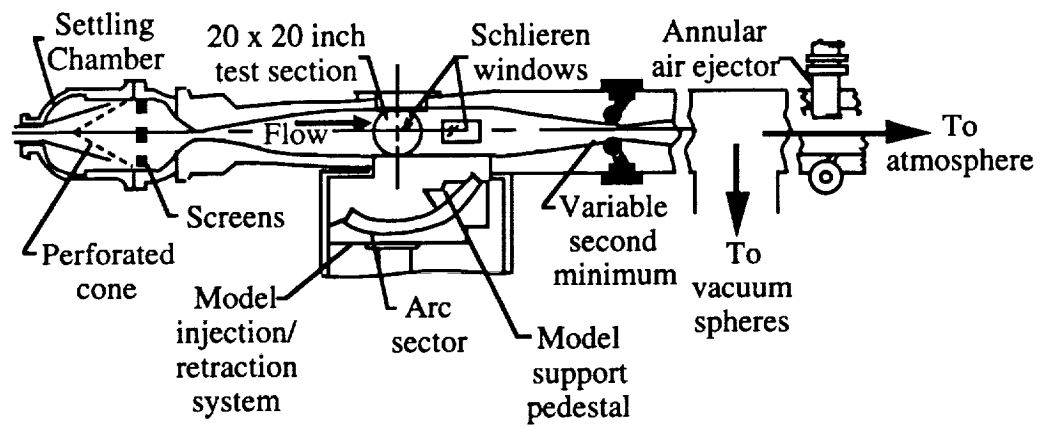
Figure 1: Two-Dimensional Inlet Model
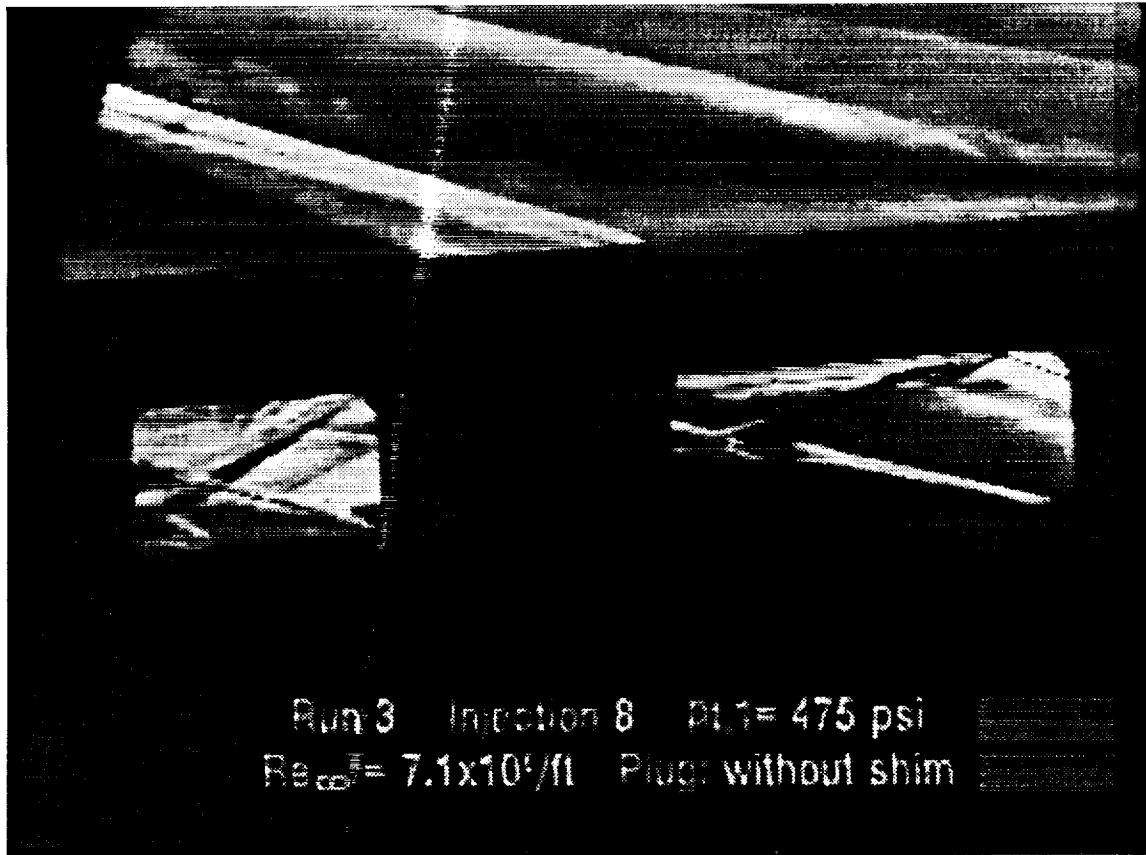
Figure 2: Schematic of 20-Inch Mach 6 Tunnel

Figure 3: Still Frame from Schlieren Video of Started Inlet in Run 3, Injection 8
Re∞=7.1 million/ft, $p_{t,1}$=475 psi, Plug Configuration: without Shim
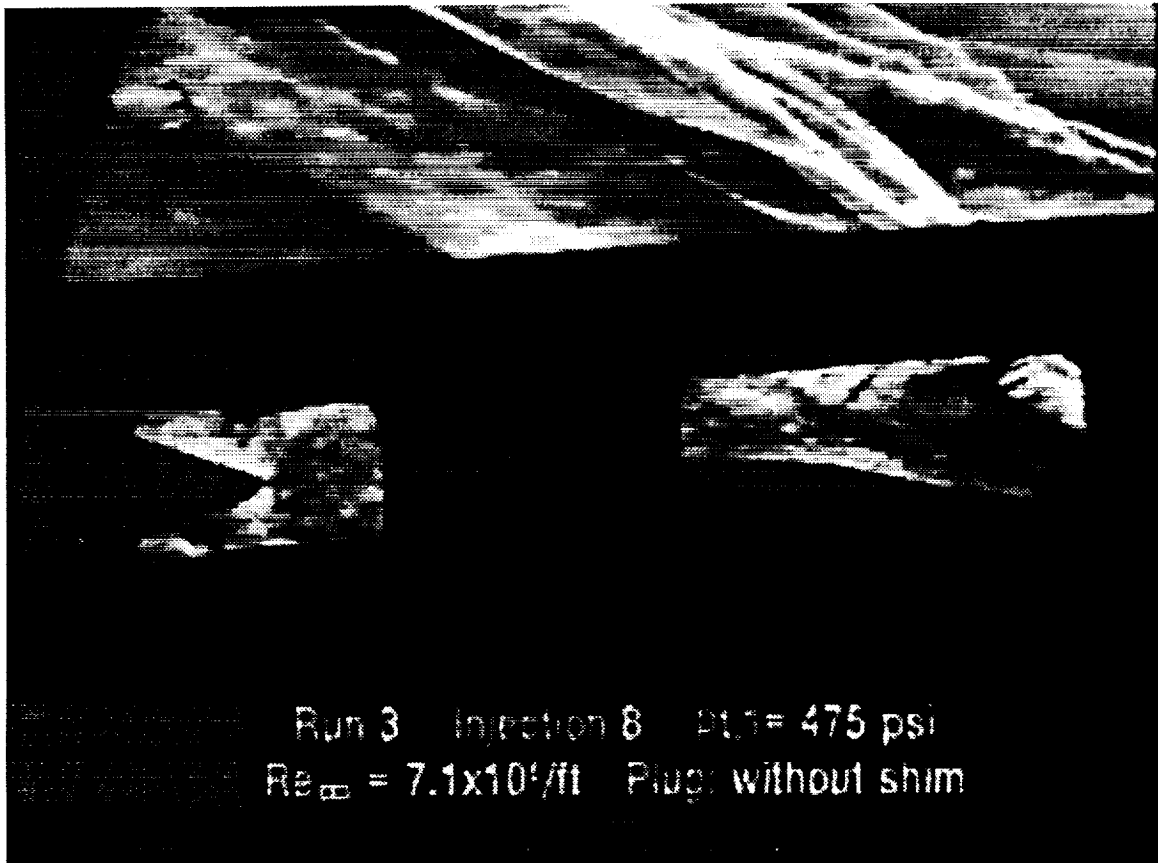Inlet Configuration: Cowl Down, Plug Aft.

Figure 4: Still Frame from Schlieren Video of Unstarted Inlet in Run 3, Injection 8
   Re_∞=7.1 million/ft, $p_{t,1}$=475 psi, Plug Configuration: without Shim
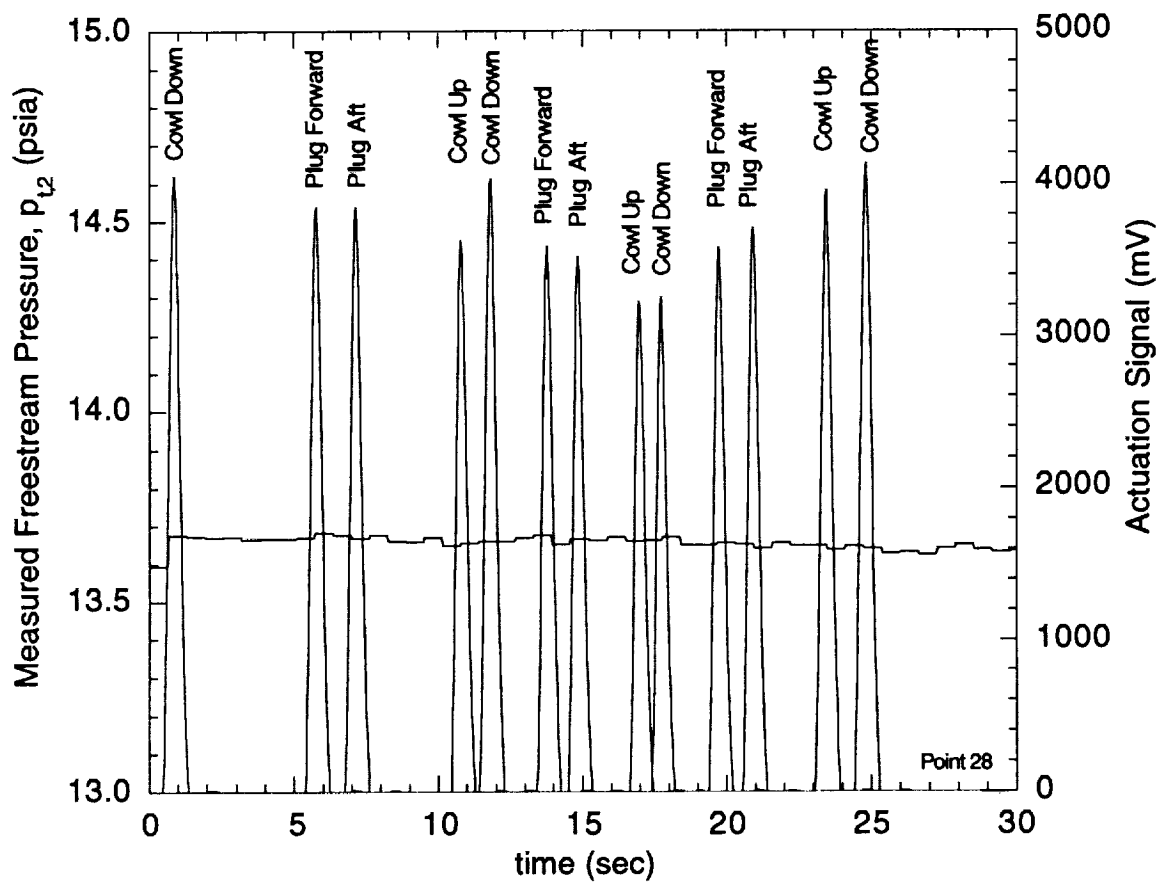   Inlet Configuration: Cowl Down, Plug Forward.

Figure 5. Effect of Cowl and Plug Position on Freestream Pitot Pressure.
Re=7.1 million/ft, Plug configured without shim (Run 3, Injection 8)

Figure 6. Effect of Cowl and Plug Position on Freestream Pitot Pressure.
Re=0.5 million/ft, Plug configured without shim (Run 3, Injection 1)

14

Figure 7. Effect of Cowl and Plug Position on Freestream Pitot Pressure.
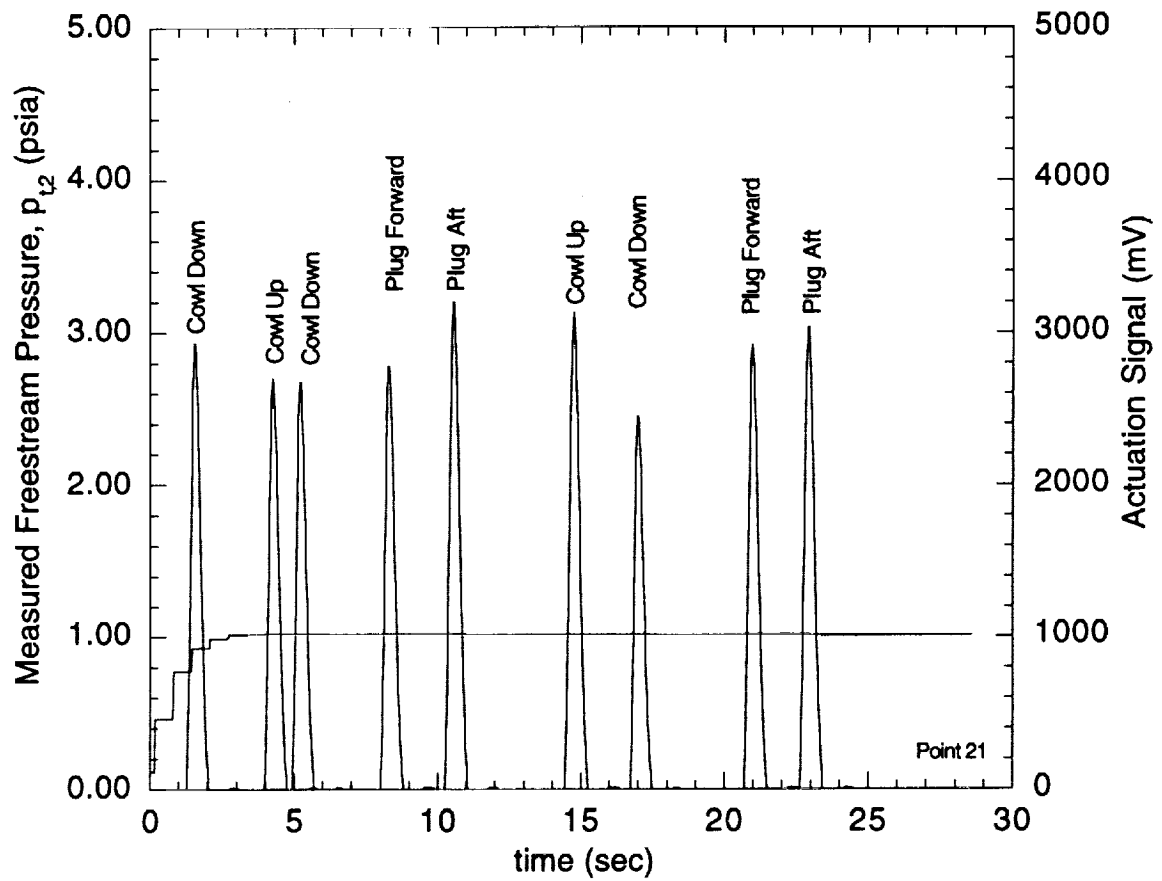Re=2.1 million/ft, Plug configured without shim (Run 3, Injection 5)

Figure 8. Effect of Cowl and Plug Position on Freestream Pitot Pressure.
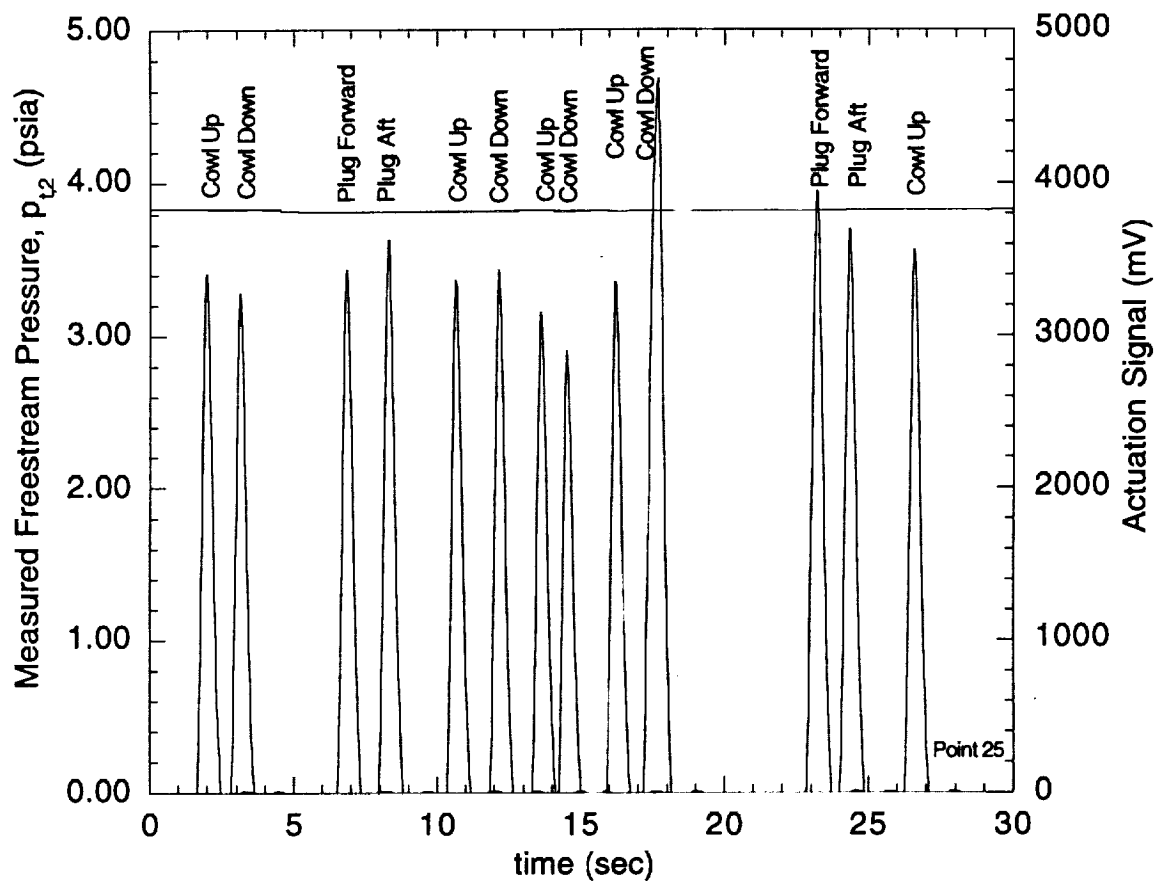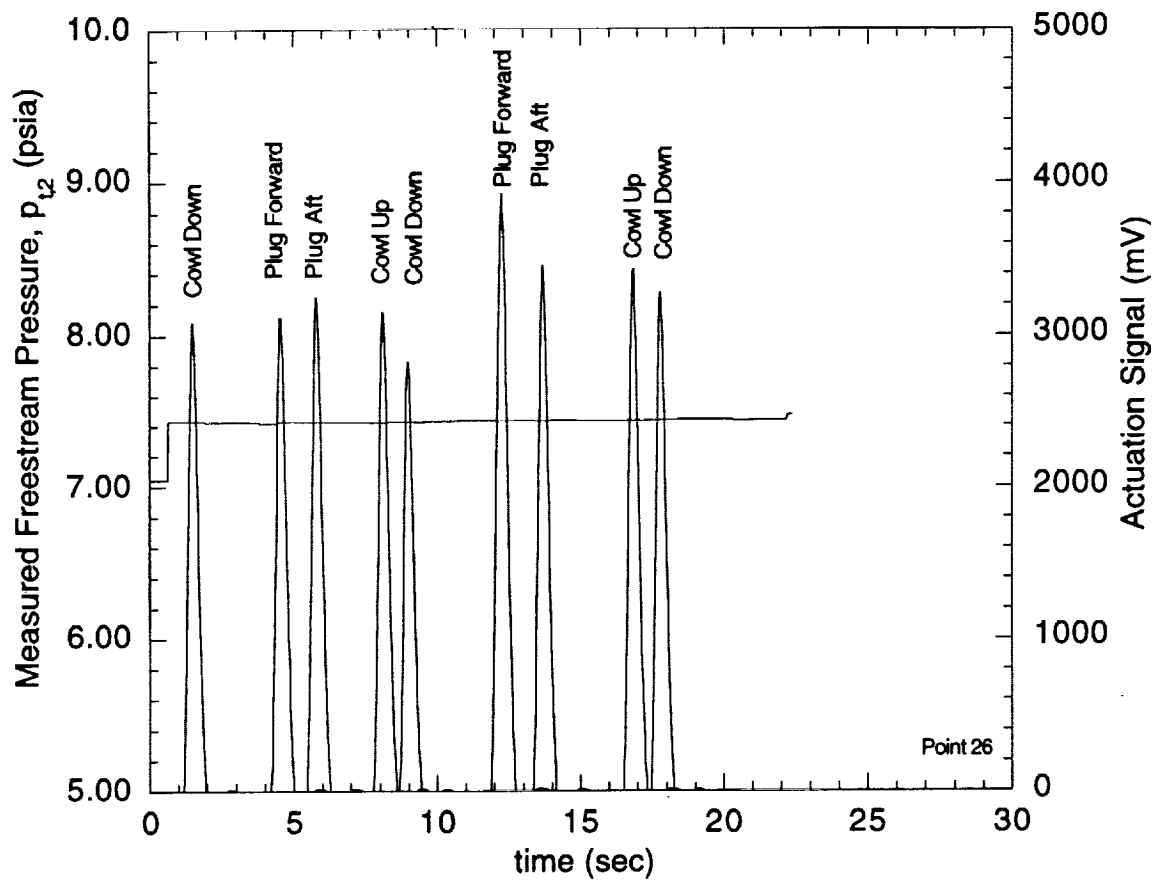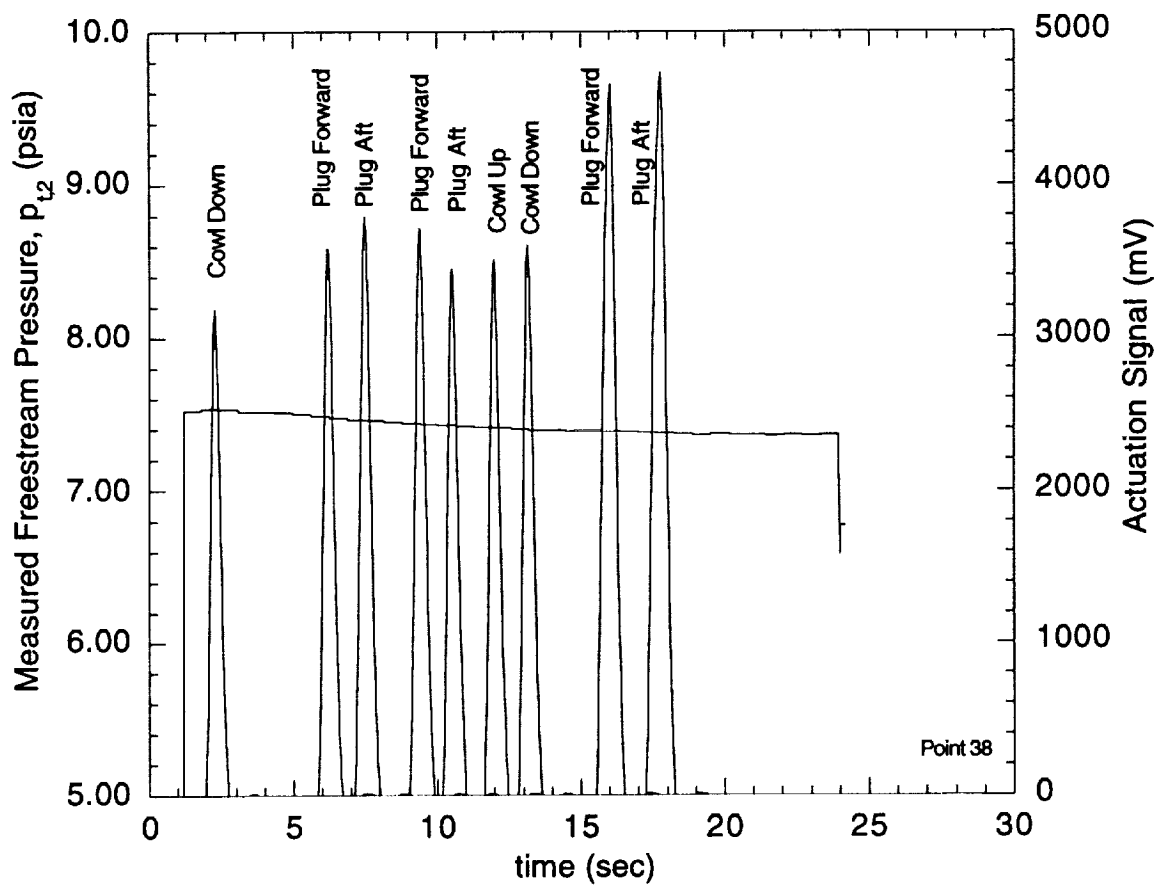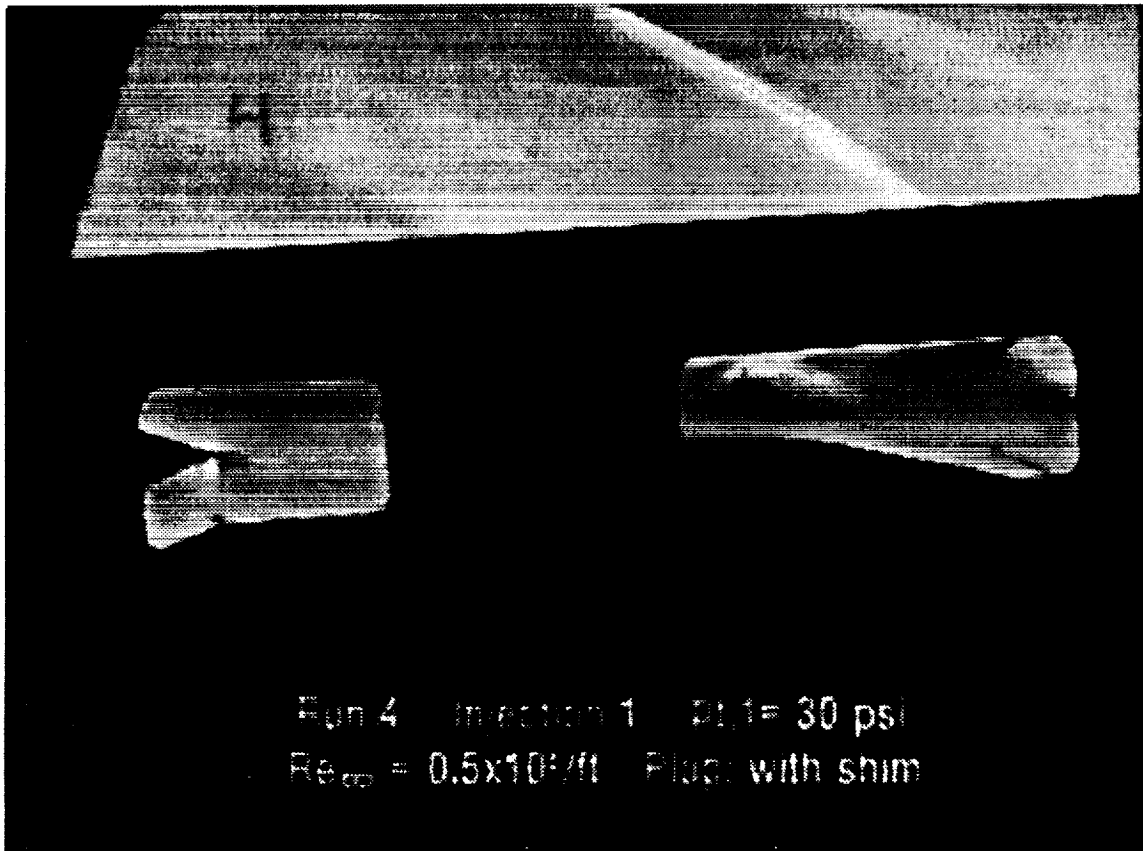Re=3.9 million/ft, Plug configured without shim (Run 3, Injection 6)

16

Figure 9. Effect of Cowl and Plug Position on Freestream Pitot Pressure.
Re=3.9 million/ft, Plug configured with shim (Run 4, Injection 5)

Figure 10: Still Frame from Schlieren Video of Unstarted Inlet in Run 4, Injection 1
Re$_\infty$=0.5 million/ft, $p_{t,1}$=30 psi, Plug Configuration: with Shim
Inlet Configuration: Cowl Down, Plug Forward.

18

Appendix A: Inlet Actuation Chronologies

A chronology of the cowl and plug actuation sequences for each model injection is provided in Tables A.1-A.22 to accompany the video supplement. In the video, flow is from right to left. The plug motion is obvious because the plug is visible in the aft window; however, the cowl is hidden from view by the inlet sidewall. The cowl actuator arm (located in the sidewall between the schlieren windows) is visible above the top of the inlet sidewalls between the windows when the cowl is up. (See figure 1b.)

Table A.1: Chronology of Run 1, Injection 1
$p_{t,1}$= 30 psi, Re_∞= 0.5 million/ft
Plug configured with shim
(Pre-run configuration: Cowl up, Plug aft)

Actuation Sequence	Comments on Inlet Flow Response
inject model	
cowl down	appears to be nominally steady but no distinct internal shock structure; external spillage evident
plug forward	internal structure never establishes; internal and external flow unsteadiness; beating
retract model	

Table A.2: Chronology of Run 1, Injection 2
$p_{t,1}$= 100 psi, Re_∞= 1.8 million/ft
Plug configured with shim
(Pre-run configuration: Cowl up, Plug forward)

Actuation Sequence	Comments on Inlet Flow Response
inject model	
cowl down	does not start; higher frequency unsteadiness than 30 psi run
retract model	

Table A.3: Chronology of Run 1, Injection 3
$p_{t,1}$= 100 psi, Re_∞= 1.8 million/ft
Plug configured with shim
(Pre-run configuration: Cowl up, Plug aft)

Actuation Sequence	Comments on Inlet Flow Response
inject model	
cowl down	external disturbance diminishes when cowl is put down; either steadier or frequency of unsteadiness is predominantly faster than video framing rate
plug forward	high frequency beating
retract model	

Table A.4: Chronology of Run 2, Injection 1
$p_{t,1}$= 100 psi, Re_∞= 1.8 million/ft
Plug configured without shim
(Pre-run configuration: Cowl up, Plug aft)

Actuation Sequence	Comments on Inlet Flow Response
inject model	
cowl down	does not start
plug forward	beating
plug aft	not started
cowl up	Character of flow oscillates. At times a larger external disturbance, at others, it is as if the inlet is trying to start with the cowl up
cowl down	inlet starts
plug forward	unstarts, unsteady beating
plug aft	does not restart
retract model	

Table A.5: Chronology of Run 2, Injection 2
$p_{t,1}$= 100 psi, Re_∞= 1.8 million/ft
Plug configured without shim
(Pre-run configuration: Cowl down, Plug aft)

Actuation Sequence	Comments on Inlet Flow Response
inject model	inlet does not start due solely to injection process
cowl up	external shock unsteadiness
cowl down	does not start, still unsteady but external disturbance smaller (less spillage), external shocks more inclined
retract model	

Table A.6: Chronology of Run 2, Injection 3
$p_{t,1}$= 250 psi, Re_∞= 3.6 million/ft
Plug configured without shim
(Pre-run configuration: Cowl up, Plug aft)

Actuation Sequence	Comments on Inlet Flow Response
inject model	large external disturbance upon injection
cowl down	inlet starts
plug forward	unstarts; very unsteady; high frequency beating
plug aft	does not restart, yet much more stable (not "beating")
retract model	

Table A.7: Chronology of Run 2, Injection 4
$p_{t,1}$= 250 psi, Re_∞= 3.6 million/ft
Plug configured without shim
(Pre-run configuration: Cowl down, Plug aft)

Actuation Sequence	Comments on Inlet Flow Response
inject model	inlet does not start due solely to injection process
plug forward	unsteadiness increases
plug aft	unsteadiness decreases
cowl up	large external disturbance
cowl down	inlet starts
plug forward	inlet unstarts; unsteady
plug aft	flow steadier but not started
cowl up	large external disturbance
cowl down	inlet starts
retract model	

22

Table A.8: Chronology of Run 3, Injection 1
$p_{t,1}$= 30 psi, Re_∞= 0.5 million/ft
Plug configured without shim
(Pre-run configuration: Cowl up, Plug aft)

Actuation Sequence	Comments on Inlet Flow Response
inject model	(zoomed schlieren installed for this and all subsequent runs)
cowl down	
cowl up	slight increase in external unsteadiness
cowl down	steadier, but not started
plug forward	slight increase in external unsteadiness
plug aft	does not start
cowl up	
cowl down	does not start
plug forward	slight increase in external unsteadiness
plug aft	does not start
retract model	

Table A.9: Chronology of Run 3, Injection 2
$p_{t,1}$= 30 psi, Re_∞= 0.5 million/ft
Plug configured without shim
(Pre-run configuration: Cowl down, Plug aft)

Actuation Sequence	Comments on Inlet Flow Response
inject model	inlet pulse started (i.e., started upon injection with the cowl down)
cowl up	
cowl down	unstarted; external shock above cowl is curved
cowl up	unsteady
cowl down	unstarted, yet steadier
retract model	

Table A.10: Chronology of Run 3, Injection 3
$p_{t,1}$= 30 psi, Re_∞= 0.5 million/ft
Plug configured without shim
(Pre-run configuration: Cowl down, Plug aft)

Actuation Sequence	Comments on Inlet Flow Response
inject model	inlet does not start upon injection with the cowl down
cowl up	unsteadiness increases
cowl down	does not started
plug forward	
plug aft	does not start
retract model	

24

Table A.11: Chronology of Run 3, Injection 4
$P_{t,1}$= 125 psi, Re_{∞}= 2.1 million/ft
Plug configured without shim
(Pre-run configuration: Cowl up, Plug aft)

Actuation Sequence	Comments on Inlet Flow Response
inject model	
cowl down	very unsteady flow; not started
plug forward	does not significantly worsen the flow characteristics
plug aft	does not significantly improve the flow characteristics
cowl up	external flow disturbance evident
cowl down	inlet starts
plug forward	unstarts; unsteady; large external interaction
plug aft	does not restart
cowl up	unsteadiness increases
cowl down	does not restart
cowl up	
cowl down	inlet starts
retract model	

Table A.12: Chronology of Run 3, Injection 5
$p_{t,1}$= 125 psi, Re_∞= 2.1 million/ft
Plug configured without shim
(Pre-run configuration: Cowl down, Plug aft)

Actuation Sequence	Comments on Inlet Flow Response
inject model	inlet does not start upon injection with the cowl down
cowl up	
cowl down	inlet starts
plug forward	inlet unstarts
plug aft	inlet does not restart
cowl up	
cowl down	inlet does not restart
cowl up	
cowl down	inlet does not restart
cowl up	
cowl down	inlet starts
plug forward	inlet unstarts
plug aft	inlet does not restart
cowl up	unsteady (beating)
retract model	

Table A.13: Chronology of Run 3, Injection 6
$p_{t,1}$= 250 psi, Re_∞= 3.9 million/ft
Plug configured without shim
(Pre-run configuration: Cowl up, Plug aft)

Actuation Sequence	Comments on Inlet Flow Response
inject model	
cowl down	inlet starts
plug forward	inlet unstarts
plug aft	does not restart
cowl up	
cowl down	inlet starts
plug forward	inlet unstarts
plug aft	does not restart
cowl up	
cowl down	inlet starts
retract model	

Table A.14: Chronology of Run 3, Injection 7
$p_{t,1}$= 250 psi, Re_∞= 3.9 million/ft
Plug configured without shim
(Pre-run configuration: Cowl down, Plug aft)

Actuation Sequence	Comments on Inlet Flow Response
inject model	does not start solely due to injection of model
cowl up	
cowl down	inlet starts
plug forward	very unsteady; large external influence
plug aft	does not restart
cowl up	
cow down	inlet starts
retract model	

28

Table A.15: Chronology of Run 3, Injection 8
$p_{t,1}$= 475 psi, Re_∞= 7.1 million/ft
Plug configured without shim
(Pre-run configuration: Cowl up, Plug aft)

Actuation Sequence	Comments on Inlet Flow Response
inject model	
cowl down	inlet starts
plug forward	unstarts; large external influence
plug aft	inlet restarts
cowl up	inlet unstarts
cowl down	inlet restarts
plug forward	inlet unstarts
plug aft	does not restart
cowl up	
cowl down	inlet starts
plug forward	inlet unstarts
plug aft	(plug movement sluggish); inlet does not restart
cowl up	
cowl down	cowl sluggish; does not restart
retract model	

Table A.16: Chronology of Run 3, Injection 9
$P_{t,1}$= 475 psi, Re_∞= 7.1 million/ft
Plug configured without shim
(Pre-run configuration: Cowl down, Plug aft)

Actuation Sequence	Comments on Inlet Flow Response
inject model	inlet pulse starts due to model injection
plug forward	inlet unstarts
plug aft	(aft plug movement very slow)
cowl up	cowl actuated up before plug was fully retracted
cowl down	inlet does not start
cowl up	
cowl down	(cowl moves very slowly); inlet does not start
retract model	

30

Table A.17: Chronology of Run 4, Injection 1
$p_{t,1}$= 30 psi, Re_∞= 0.5 million/ft
Plug configured with shim
(Pre-run configuration: Cowl up, Plug aft)

Actuation Sequence	Comments on Inlet Flow Response
inject model	
cowl down	external influence decreased, but inlet has not started
cowl up	
cowl down	does not start
plug forward	low frequency beating
plug aft	not started but steadier
cowl up	
cowl down	does not start
retract model	

Table A.18: Chronology of Run 4, Injection 2
$p_{t,1}$= 30 psi, Re_∞= 0.5 million/ft
Plug configured with shim
(Pre-run configuration: Cowl down, Plug aft)

Actuation Sequence	Comments on Inlet Flow Response
inject model	inlet does not pulse start due to model injection
cowl up	
cowl down	inlet does not start
cowl up	
retract model	

31

Table A.19: Chronology of Run 4, Injection 3
$p_{t,1}$= 125 psi, Re_∞= 2.2 million/ft
Plug configured with shim
(Pre-run configuration: Cowl up, Plug aft)

Actuation Sequence	Comments on Inlet Flow Response
inject model	
cowl down	inlet does not start
cowl up	
cowl down	inlet does not start
plug forward	large unsteady forward influence, but not quite like beating previously noted. (Beating = when the entire flow structure moves in/out together. This was more ragged.)
plug aft	inlet does not start
cowl up	
cowl down	inlet does not start
retract model	

Table A.20: Chronology of Run 4, Injection 4
$p_{t,1}$= 125 psi, Re_∞= 2.2 million/ft
Plug configured with shim
(Pre-run configuration: Cowl down, Plug aft)

Actuation Sequence	Comments on Inlet Flow Response
inject model	inlet does not pulse start
cowl up	flow unsteadiness increases
cowl down	flow is steadier but not started
cowl up	flow unsteadiness increases
cowl down	flow is steadier but not started
retract model	

33

Table A.21: Chronology of Run 4, Injection 5
$p_{t,1}$= 250 psi, Re_∞= 3.9 million/ft
Plug configured with shim
(Pre-run configuration: Cowl up, Plug aft)

Actuation Sequence	Comments on Inlet Flow Response
inject model	
cowl down	inlet starts
plug forward	inlet unstarts
plug aft	inlet restarts
plug forward	inlet unstarts
plug aft	inlet restarts
cowl up	unstarts; plug appears to droop due to download when cowl is raised
cowl down	inlet does not restart
plug forward	(plug motion very slow)
plug aft	(plug motion very slow); inlet does not restart
retract model	

34

Table A.22: Chronology of Run 5, Injection 1
$p_{t,1}$= 475 psi, Re_{∞}= 7.1 million/ft
Plug configured with shim
(Pre-run configuration: Cowl down, Plug aft)

Actuation Sequence	Comments on Inlet Flow Response
NOTE:	Plug actuation rod broke during a previous run. Rod was replaced prior to this run
inject model	inlet does not pulse start; large external influence is noted
cowl up	
cowl down	inlet does not start
cowl up	(plug droops); inlet does not start
retract model	

Video supplement L-0194-41 is available for purchase.

This video (11 minutes, color, VHS) shows the schlieren video of the external flow field and a portion of the internal flow field for each model injection sequence, as documented in this report.

To obtain the video, fill out the mail-in card below and return it to:

ATTN USER SERVICES
NASA CENTER FOR AEROSPACE INFORMATION
P.O. BOX 8757
BALTIMORE, MD 21240-0757

Cut here -

Please send ___ copies of video supplement L-0194-41 to NASA TM 109152.

Attn: _____
        Name

        _____
        Title

        _____
        Organization

        _____
        Street Address

        _____
        City and State   Zip Code

REPORT DOCUMENTATION PAGE		Form Approved OMB No. 0704-0188

1. AGENCY USE ONLY (Leave blank)	2. REPORT DATE November 1994	3. REPORT TYPE AND DATES COVERED Technical Memorandum

4. TITLE AND SUBTITLE

Wind-Tunnel Blockage and Actuation Systems Test of a Two-Dimensional Scramjet Inlet Unstart Model at Mach 6

5. FUNDING NUMBERS

WU 763-23-35-08

6. AUTHOR(S)

Scott D. Holland

7. PERFORMING ORGANIZATION NAME(S) AND ADDRESS(ES)

NASA Langley Research Center
Hampton, VA 23681-0001

8. PERFORMING ORGANIZATION REPORT NUMBER

9. SPONSORING/MONITORING AGENCY NAME(S) AND ADDRESS(ES)

National Aeronautics and Space Administration
Washington, DC 20546-0001

10. SPONSORING/MONITORING AGENCY REPORT NUMBER

NASA TM 109152

11. SUPPLEMENTARY NOTES

Video Supplement Available as L-0194-41

12a. DISTRIBUTION/AVAILABILITY STATEMENT

Unclassified-Unlimited

Subject Category 34

12b. DISTRIBUTION CODE

13. ABSTRACT (Maximum 200 words)

The present study examines the wind-tunnel blockage and actuation systems effectiveness in starting and forcibly unstarting a two-dimensional scramjet inlet in the NASA Langley 20-Inch Mach 6 Tunnel. The intent of the overall test program is to study (both experimentally and computationally) the dynamics of the inlet unstart; however, prior to the design and fabrication of an expensive, instrumented wind-tunnel model, it was deemed necessary first to examine potential wind-tunnel blockage issues related to model sizing and to examine the adequacy of the actuation systems in accomplishing the start and unstart. The model is equipped with both a moveable cowl and aft plug. Windows in the inlet sidewalls allow limited optical access to the internal shock structure; schlieren video was used to identify inlet start and unstart. A chronology of each actuation sequence is provided in tabular form along with still frames from the schlieren video. A pitot probe monitored the freestream conditions throughout the start/unstart process to determine if there was a blockage effect due to the model start or unstart. Because the purpose of this report is to make the phase I (blockage and actuation systems) data rapidly available to the community, the data is presented largely without analysis of the internal shock interactions or the unstart process. This series of tests indicated that the model was appropriately sized for this facility and identified operability limits required first to allow the inlet to start and second to force the unstart.

14. SUBJECT TERMS Hypersonics; Inlets; Unstart; Shock Interactions	15. NUMBER OF PAGES 37
	16. PRICE CODE A03

17. SECURITY CLASSIFICATION OF REPORT Unclassified	18. SECURITY CLASSIFICATION OF THIS PAGE Unclassified	19. SECURITY CLASSIFICATION OF ABSTRACT	20. LIMITATION OF ABSTRACT